

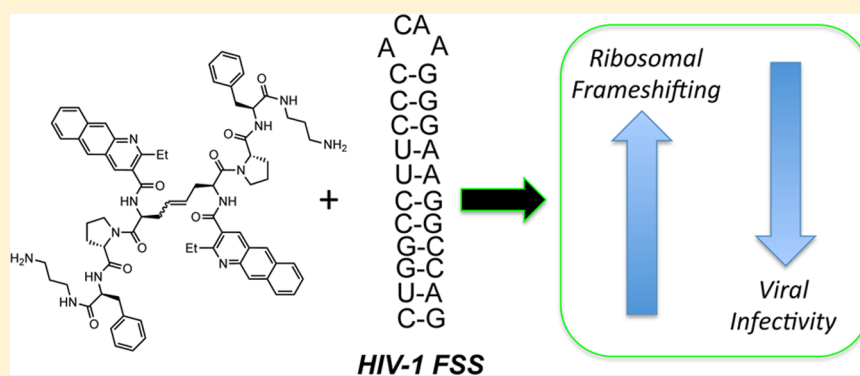
## High-Affinity Recognition of HIV-1 Frameshift-Stimulating RNA Alters Frameshifting in Vitro and Interferes with HIV-1 Infectivity

Leslie O. Ofori,<sup>†,||</sup> Thomas A. Hilimire,<sup>‡,||</sup> Ryan P. Bennett,<sup>⊥,||</sup> Nathaniel W. Brown, Jr.,<sup>†</sup> Harold C. Smith,<sup>⊥,‡</sup> and Benjamin L. Miller\*,<sup>†,‡,§</sup>

<sup>†</sup>Departments of Chemistry, <sup>‡</sup>Biochemistry and Biophysics, and <sup>§</sup>Dermatology, University of Rochester, Rochester, New York 14642, United States

<sup>⊥</sup>Oyagen, Inc., Henrietta, New York 14623, United States

### Supporting Information



**ABSTRACT:** The life cycle of the human immunodeficiency virus type 1 (HIV-1) has an absolute requirement for ribosomal frameshifting during protein translation in order to produce the polyprotein precursor of the viral enzymes. While an RNA stem-loop structure (the “HIV-1 Frameshift Stimulating Signal”, or HIV-1 FSS) controls the frameshift efficiency and has been hypothesized as an attractive therapeutic target, developing compounds that selectively bind this RNA and interfere with HIV-1 replication has proven challenging. Building on our prior discovery of a “hit” molecule able to bind this stem-loop, we now report the development of compounds displaying high affinity for the HIV-1 FSS. These compounds are able to enhance frameshifting more than 50% in a dual-luciferase assay in human embryonic kidney cells, and they strongly inhibit the infectivity of pseudotyped HIV-1 virions.

### INTRODUCTION

Human immunodeficiency virus type 1 (HIV-1), the causative agent of acquired immune deficiency syndrome (AIDS), remains a significant challenge to global health.<sup>1,2</sup> Since its initial identification in 1983, HIV-1 infection has reached the status of a pandemic. In 2009 alone, there were approximately 2.7 million new infections and about 2.0 million deaths from AIDS related causes.<sup>3</sup> Currently there is no cure for HIV-1 infection. While progression of the disease can be controlled by highly active antiretroviral therapy (HAART), a combination of drugs designed to inhibit different stages in the virus’ life cycle,<sup>4</sup> the complexity of the HAART regimen, and the ability of the virus to evolve resistance suggest that alternative drug targets for HIV-1 treatment and prophylaxis are needed.<sup>5</sup>

One potentially attractive target for pharmacological interference in the HIV-1 life cycle is the virus’ requirement for a programmed –1 ribosomal frameshift (–1 PRF) in order to express its enzymes.<sup>6</sup> Ribosomal frameshifting is a recoding mechanism common among viruses with polycistronic (multiple open reading frames, or ORFs, in a single gene) genomes. It allows viruses to translate polypeptides in different ORFs by

avoiding the stop codon(s) present in the single mRNA transcript. In HIV-1, the *pol* gene is in the –1 reading frame with respect to *gag*. *Gag*, the precursor of the viral structural proteins, is produced via normal translational rules, while *Pol*, the precursor of the viral enzymes, is synthesized as a fused *Gag-Pol* polyprotein via –1 PRF. This occurs with a frequency of 5–10% of ribosomes translating the full-length viral mRNA. A critical molar ratio of *Gag-Pol* to *Gag* protein is required for HIV-1 replication and infectivity; alterations to this ratio have been shown to be detrimental.<sup>7</sup> –1 PRF in HIV-1 is controlled by two *cis* acting mRNA elements: a heptameric slippery sequence (U UUU UUA), with the 0 frame indicated by spaces and where the frameshift actually occurs, and a downstream two-stem helix immediately following the slippery sequence, also known as the frameshift stimulatory signal (HIV-1 FSS, Figure 1).<sup>8</sup> While several mechanisms have been proposed to account for the frameshift,<sup>9</sup> it is currently hypothesized that this event results from an incomplete translocation for a limited

Received: September 17, 2013

Published: January 5, 2014



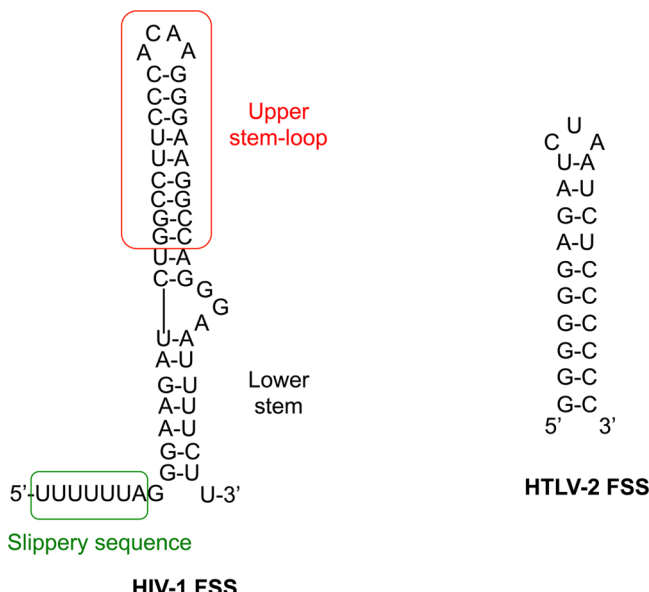


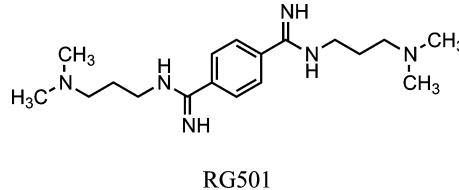
**Figure 1.** HIV-1 and HTLV-2 FSS RNAs. (Left) Proposed secondary structure of the HIV-1 FSS, supported by NMR structural studies. (Right) HTLV-2 FSS stem-loop sequence used as a specificity control in this work. Note that when the slippery sequence occupies the decoding site of the ribosome, the lower stem is unwound and it is the upper stem-loop that acts as the effective frameshift stimulatory signal.

number of ribosomes, due to resistance of the FSS to unwinding.<sup>10–12</sup> These ribosomes then start translation of *pol* in the new –1 reading frame. Modification of the slippery site or stimulatory sequence (either via natural variation or laboratory mutations) in ways affecting frameshifting efficiency translates to a decrease in viral replication.<sup>13,14</sup> These and other results have led several groups to propose –1 PRF as a potential target for developing antiretroviral agents for HIV-1.<sup>6,15–17</sup>

NMR structural analyses indicate that the HIV-1 FSS RNA consists of a G-C rich upper stem-loop structure,<sup>18</sup> separated from a flexible lower stem by a GGA trinucleotide bulge (Figure 1).<sup>19,20</sup> The bulge produces a roughly 60° bend between the upper and lower stems. The upper stem-loop is exceptionally stable. This stability is believed to play a vital role in the stimulation of the frameshift, since the ribosome must unwind the stem during translation. The lower stem is thermodynamically less stable. The highly structured ACAA tetraloop is uncommon among tetraloops<sup>21</sup> but is conserved among all HIV-1 group M subtypes except the uncommon H and J subtypes. Likewise, the heptameric slippery sequence is conserved across all HIV-1 group M subtypes. SHAPE analysis of the intact HIV genome suggests a more complex structure for the FSS RNA, although the upper stem-loop is retained.<sup>22,23</sup>

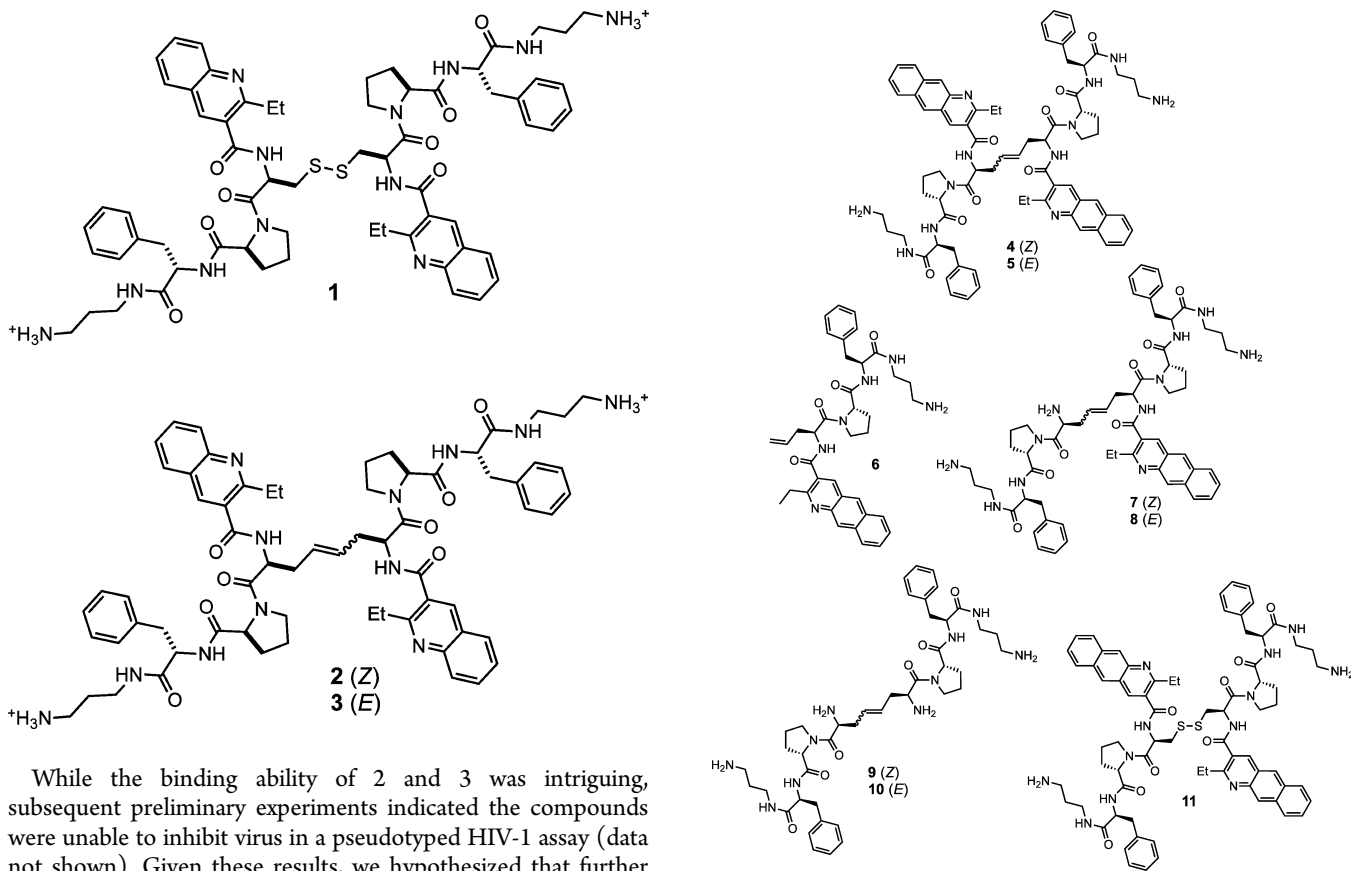
Since other viruses also rely on frameshifting,<sup>24</sup> targeting frameshift-regulating structures may have general utility beyond the context of HIV. For example, human T-cell leukemia virus type 2 (HTLV-2) uses two –1 PRF events similar to HIV-1 in order to synthesize fused Gag-Pro and Gag-Pro-Pol precursor proteins.<sup>25</sup> The RNA responsible for the –1 PRF essential for expression of Gag-Pro in HTLV-2 also consists of two *cis*-acting RNA elements, a heptanucleotide (AAAAAAC) slippery site and a stem-loop shown in Figure 1.<sup>26</sup> This HTLV-2 FSS served as a sequence specificity control in the experiments we describe herein.

The first attempted use of a synthetic molecule to alter HIV-1 frameshifting and thereby influence viral replication was reported by Green and co-workers in 1998.<sup>27</sup> The authors showed that 1,4-bis[N-(3-N,N-dimethylpropyl)amidino]-benzene tetrahydrochloride, a bis guanidinium-containing compound termed “RG501”, was able to stimulate –1



frameshifting, alter the Gag-Pol:Gag ratio, inhibit HIV-1 replication in CEM cells (a lymphocytic cell line), and interfere with the formation of viral particles in chronically infected CH-1 cells (a COS cell line stably transfected with HIV-gpt, an HIV derivative in which the *E. coli gpt* gene replaces HIV *env*).<sup>28</sup> Increases in reverse transcriptase (RT) following treatment with 1.5 mM RG501 were also observed, as would be expected for an increase in Gag-Pol production. Recently, the Butcher group confirmed that this compound indeed binds the HIV-1 FSS RNA with weak affinity ( $K_D \sim 360 \mu\text{M}$ ), and they carried out NMR structure analysis, indicating that RG501 binds in the major groove of the upper stem-loop.<sup>29</sup> Unfortunately, as noted by the authors, RG501 is a relatively nonselective binder and interacts with other RNAs. It stimulates frameshifting in viruses with different FSS,<sup>29</sup> and likely that also interacts with the ribosome.<sup>6</sup> RG501 is also toxic,<sup>27</sup> a likely result of its lack of selectivity. Moreover, its interference with HIV replication begins at concentrations below those observed to affect frameshifting.<sup>27,24</sup> Other compounds such as guanidinoneomycin,<sup>30</sup> idarubicin, and doxorubicin<sup>31</sup> have been shown to bind the HIV-1 FSS. Doxorubicin was found to bind with a  $K_D$  of 2.8  $\mu\text{M}$ , decreased frameshifting in a rabbit reticulocyte assay, and also significantly reduced overall translation. A screen of an Arg-rich peptide library revealed a sequence able to significantly reduce frameshifting, but this displayed no selectivity for the HIV-1 FSS relative to other frameshift-stimulating constructs and likely also interacts with the ribosome.<sup>32</sup> Thus, as far as we are aware, there are no reported examples of synthetic molecules able to alter HIV-1 frameshifting and interfere with viral infectivity via selective, high-affinity binding to the FSS RNA.

Building on our laboratory’s longstanding interest in understanding the factors that drive affinity and sequence selectivity in small molecule recognition of RNA,<sup>33</sup> we previously reported the use of an 11,325-member resin-bound dynamic combinatorial library<sup>34</sup> (designed based on the structure of DNA-binding, bisintercalating peptide antibiotics) to identify a compound (1) able to bind the HIV-1 FSS upper stem-loop with moderate affinity ( $K_D = 4.1 \pm 2.4 \mu\text{M}$ ) immobilized on an surface plasmon resonance (SPR) chip via one of its amine groups;  $K_D = 350 \pm 110 \text{ nM}$  in solution as measured by fluorescence<sup>35</sup>) and good selectivity.<sup>36</sup> Subsequent efforts revealed that replacement of the disulfide bridge with an olefin (to produce compounds 2 and 3) could be accomplished without any reduction in affinity. These studies also indicated that affinity was essentially abolished if the  $\pi$ -surface area of the molecule was reduced, while the peptidic portion of 1 was required for sequence-selective binding.<sup>35</sup>



While the binding ability of 2 and 3 was intriguing, subsequent preliminary experiments indicated the compounds were unable to inhibit virus in a pseudotyped HIV-1 assay (data not shown). Given these results, we hypothesized that further increases in affinity were essential. We anticipated that increasing the  $\pi$  surface area of 1 could represent a viable strategy for enhancing the affinity for the HIV-1 FSS without significant reductions in selectivity. In particular, incorporation of a benzo[g]quinoline moiety to produce 4 and 5 was viewed as attractive. This hypothesis was supported in part by parallel efforts in our laboratory on the design and synthesis of compounds targeting CUG repeat RNA in which incorporation of a benzo[g]quinoline was found to enhance affinity and to provide compounds with activity *in vivo* in a mouse model of Type 1 Myotonic Dystrophy.<sup>37</sup> Synthesis of 4 and 5 proceeded via cross-metathesis of half-structure 6, by analogy to our previous work. We also synthesized 7 and 8 (“one-armed” benzo[g]quinoline-bearing structures), as well as compounds 9 and 10, to test the effect of sequential removal of the putative

intercalators. Compound 11 was synthesized in order to ascertain the effectiveness of the olefin bioisostere in improving cellular availability and bioactivity relative to an easily reduced disulfide.

## RESULTS AND DISCUSSION

Synthesized compounds were first analyzed for binding to the HIV-1 FSS by surface plasmon resonance (SPR). This technique allows the equilibrium constant ( $K_D$ ) and kinetic rate constants ( $k_{on}$ ,  $k_{off}$ ) to be determined in a label-free format.<sup>38</sup> A 5'-biotin labeled HIV-1 FSS RNA upper stem-loop (sequence as in Figure 1) was immobilized on a streptavidin-functionalized sensor chip. Compound solutions in HBS buffer (0.01 M HEPES, 0.150 M NaCl, pH = 7.4) were flowed over

**Table 1. Binding Constants and Binding Rate Constants for Benzo[g]quinoline-Containing Analogs of Compound 3 to the HIV-1 FSS Measured by SPR<sup>a</sup>**

compd	conditions <sup>a</sup>	association rate, $k_a$ ( $M^{-1}s^{-1}$ )	dissociation rate $k_d$ ( $s^{-1}$ )	dissociation constant, $K_D$ ( $\mu M$ )
3	a	$1.62 \times 10^3$	$7.5 \times 10^{-3}$	4.66
4	a	$(4.25 \pm 0.22) \times 10^4$	$(4.11 \pm 0.02) \times 10^{-3}$	0.102
5	a	$(3.99 \pm 0.37) \times 10^4$	$(3.75 \pm 0.12) \times 10^{-3}$	0.089
6	a	$(1.16 \pm 0.06) \times 10^3$	$(2.25 \pm 0.01) \times 10^{-2}$	19.5
7	a	$(4.58 \pm 1.27) \times 10^3$	$(1.21 \pm 0.00) \times 10^{-2}$	2.76
8	a	$(7.71 \pm 4.9) \times 10^3$	$(1.63 \pm 1.12) \times 10^{-1}$	20.7
10	a, b	none obsd	none obsd	none obsd
11	a	$(1.07 \pm 0.07) \times 10^4$	$(7.92 \pm 0.53) \times 10^{-3}$	0.741
4	b	$(2.17 \pm 0.77) \times 10^4$	$(1.35 \pm 0.03) \times 10^{-3}$	0.071
5	b	$(3.68 \pm 1.45) \times 10^4$	$(3.46 \pm 2.05) \times 10^{-3}$	0.096

<sup>a</sup>Error represents standard error on the global fit of at least five sensorgrams. Compound injection was repeated twice at each concentration to verify consistency. Data for compound 3 is from ref 35. Conditions: (a) HBS buffer (0.01 M HEPES, 0.150 M NaCl, pH = 7.4); (b) 20 mM HEPES, 150 mM NaCl, 5 mM MgCl<sub>2</sub>, and 0.005% Tween-20.

the RNA, and the reference-subtracted sensorgrams were recorded. The associative and dissociative phases of the experimental sensorgrams for at least five different concentrations were globally fit to a 1:1 Langmuir equation to obtain the binding constants.<sup>39</sup>

Under these conditions, benzo[g]quinoline-containing compounds 4 and 5 bound the HIV-1 FSS with affinities ( $K_D$ ) of 89 nM and 102 nM, respectively, in each case representing an approximately 50-fold increased affinity over 2 and 3 (Table 1). Binding by benzo[g]quinoline containing monomer 6 was 200-fold weaker relative to that of the dimers 4 and 5. Removal of one heterocycle “arm” also resulted in an approximately 200-fold decrease in affinity for 7 and a 30-fold decrease for 8, while removal of both benzo[g]quinoline groups completely abrogated binding between 10 and the HIV-1 FSS RNA, consistent with our prior results, indicating the importance of the heterocyclic group for affinity. Disulfide linked compound 11 bound the target RNA with a  $K_D$  of 0.741  $\mu$ M, which is ~7-fold weaker relative to the olefin analogs 4 and 5. No binding was observed between the 2-ethyl benzo[g]quinoline carboxylic acid and the HIV-1FSS by SPR. Confirming their anticipated selectivity for the HIV-1 FSS, compounds 4–10 showed no binding to the HTLV-2 FSS by SPR at concentrations up to 3  $\mu$ M (Supporting Information p S12).

The dissociation phase for SPR traces obtained at the highest concentrations for compounds 4 and 5 were not well fit by a single-exponential function. To control for the possibility of compound aggregation interfering with the measurement,<sup>40</sup> we therefore reexamined these compounds using a running buffer containing detergent (20 mM HEPES, 150 mM NaCl, 5 mM MgCl<sub>2</sub>, and 0.005% Tween-20). This had only a marginal impact on the fitted kinetic parameters (Table 1), suggesting aggregation is not a significant complicating factor in the assay. An SPR chip with a very low density of RNA provided similar dissociation constants (Supporting Information).

To confirm thermodynamic dissociation constants measured by SPR with a fully solution-phase method, and to further assess sequence selectivity, fluorescence titrations were conducted. In these experiments, saturable quenching of benzo[g]quinoline fluorescence was observed as a function of added unlabeled RNA. Dissociation constants obtained in this manner (Table 2) for 4 and 5 binding the HIV-1 FSS RNA are in general agreement with those obtained via SPR. By fluorescence we observe a 5-fold selectivity for 4 binding the FSS RNA vs total yeast tRNA, while selectivity for FSS RNA vs FSS DNA was 4-fold. The selectivity of 5 for FSS RNA vs tRNA was somewhat lower (2.14-fold). Curiously, unlike 4, 5

had no selectivity for FSS RNA vs FSS DNA. Thus, as 2 and 3 were previously found to have no measurable affinity for tRNA, we conclude that the increase in affinity obtained on replacement of the quinoline moieties of 2 and 3 with benzo[g]quinoline does come with a cost of some decrease in selectivity. This result is in contrast to what was observed in a related series of compounds optimized for binding triplet repeat RNA sequences relevant to type 1 myotonic dystrophy.<sup>37</sup> It is likely that these differences have a structural foundation, and further experiments will be needed to explore this hypothesis.

**Cell Permeation and Toxicity.** Before analyzing the effect of compounds on HIV-1 frameshifting in cells, we verified that they were capable of crossing cell membranes, and not toxic at reasonable concentrations. Human embryonic kidney cells (HEK 293FT) were treated with 4, 5, and 11 at concentrations of 50, 100, 200, and 500  $\mu$ M for 12 h. Cells were then washed using standard methods<sup>41</sup> to ensure that cell staining was not simply due to surface capture. The inherent fluorescence of the benzo[g]quinoline chromophore in these compounds allowed direct visualization of cell penetration via fluorescence microscopy (Figure 2 shows results for 50  $\mu$ M treatment; additional images are provided in the Supporting Information), confirming that cells internalized all three compounds. Compounds did not appear to localize in any specific

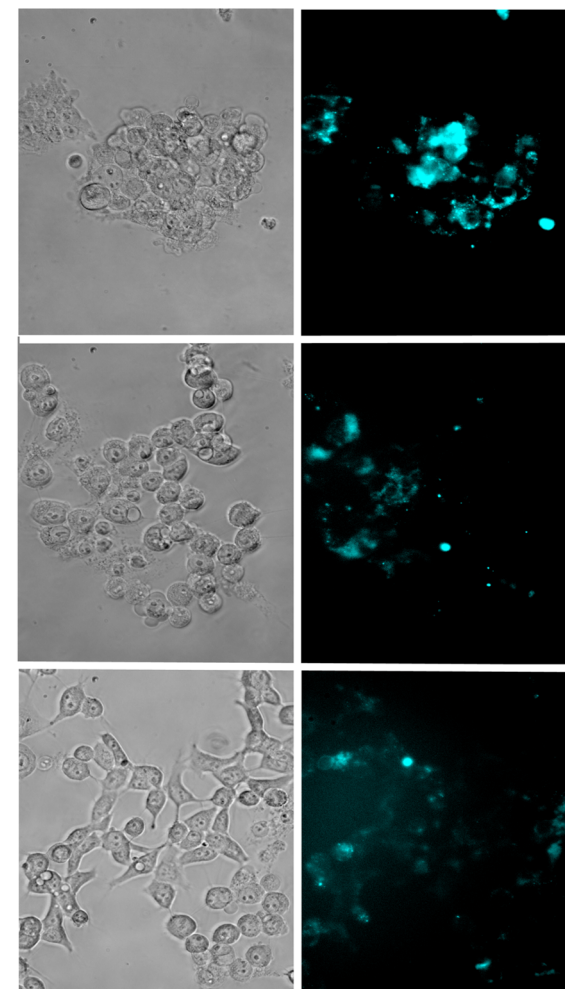


**Figure 2.** HIV-1 FSS ligands are cell permeable. Bright-field (gray) and false-color fluorescence images of compound 4, 5, and 11 incubated with HEK 293FT cells at a concentration of 50  $\mu$ M.

**Table 2. Binding Constants Measured by Fluorescence Titration for Compounds 4–6 in 20 mM HEPES with 150 mM NaCl<sup>a</sup>**

compd	sequence	$K_D$ (nM)
4	FSS RNA	66 ± 34
4	tRNA	334 ± 28
4	FSS DNA	265 ± 38
5	FSS RNA	101 ± 29
5	tRNA	217 ± 27
5	FSS DNA	118 ± 20
6	FSS RNA	409 ± 25

<sup>a</sup>Reported error is the standard deviation on each measurement taken in triplicate with 1 min spacing between measurements.

subcellular structures but were visible throughout the cytoplasm and nucleus.

Cell viability was analyzed using the WST-1 assay.<sup>42</sup> Compounds were incubated with HEK 293FT cells cultured in DMEM for 24 h, after which a 10:1 media to WST-1 cell proliferation reagent mixture replaced the growth media for 2 h. Absorbance was then measured at 450 and 690 nm. Disulfide linked compound 11 proved toxic at concentrations above 10  $\mu\text{M}$ , while no significant toxicity for compounds 4 and 5 occurred at concentrations below 60  $\mu\text{M}$  (Figure 3). The higher toxicity observed for 11 relative to 4 and 5 is not surprising and likely reflects the lability of the disulfide bond in the reducing environment of the cell.

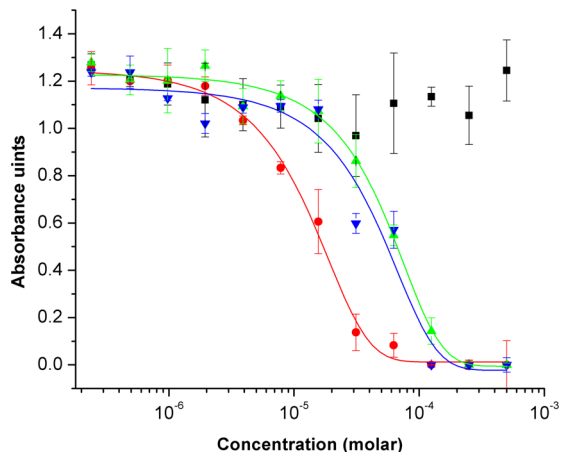


**Figure 3.** Toxicity of HIV-1 FSS ligands in HEK 293FT cells, assessed via WST-1 cell proliferation assay. Results are shown for exposure to 4 (blue triangles), 5 (green triangles), or 11 (red circles), in comparison to addition of buffer alone (black squares). Lines are provided only to guide the eye. The error on each data point is the standard deviation on three measurements.

**Dual-Luciferase Frameshift Assay in HEK 293 FT Cells.** Compounds were next evaluated for their ability to alter HIV-1 FSS-dependent frameshifting, using a dual-luciferase reporter assay.<sup>43</sup> In this system, the FSS sequence has been inserted between *Renilla* (Rluc) and firefly (Fluc) luciferase genes. Several constructs were employed. In the pDualHIV(−1) construct, Fluc is in the −1 reading frame relative to Rluc, while, in the pDualHIV(0) construct, Fluc is in the 0 reading frame relative to Rluc. In both cases, Fluc is expressed only as a fused Rluc-Fluc protein, but in the case of pDualHIV(−1), a −1 frameshift is required. To ascertain if compound-dependent effects on frameshifting are specific to HIV-1, we also carried out an analogous −1 PRF assay using constructs in which the HTLV-2 frameshift site<sup>44</sup> was inserted between Rluc and Fluc genes, such that Fluc is only synthesized by a −1PRF event [pDualHTLV-2 (−1)].<sup>45</sup>

HEK 293FT cells were transiently transfected separately with pDualHIV(−1) and pDualHIV(0) plasmids. The frameshift efficiency (defined as the ratio of firefly to *Renilla* luciferase activities) in the pDualHIV(−1) transfected cells was measured in the presence of varying concentrations of compounds (0–50  $\mu\text{M}$ ). A statistically significant ( $p < 0.005$ ) dose-dependent increase in Fluc to Rluc ratios, >50% at 50  $\mu\text{M}$ , was observed following treatment with 4 or 5 (Figure 4). Control compound 10, which showed no measurable binding to the HIV-1 FSS by SPR, had no significant effect on −1 PRF in pDualHIV(−1)

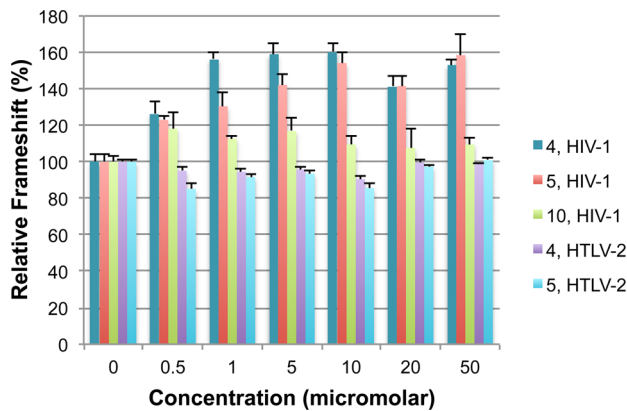


**Figure 4.** Compounds 4 and 5 increase frameshifting (>50%) in a dual-luciferase assay incorporating the HIV-1 FSS but have no effect on frameshifting in analogous assay incorporating the HTLV-2 FSS. Relative frameshift efficiency in HEK 293FT cells treated with 4, 5 or control peptide 10 after transfection with pDualHIV (−1) or pDualHTLV-2 (−1). The frameshift efficiency was calculated as the ratio of Fluc to Rluc in pDualHIV(−1) or pDualHTLV-2 (−1) transiently transfected cells. This ratio was arbitrarily set to 100% for plasmid-transfected cells, but not exposed to compounds. Error is SEM on three replicates for each concentration.

transfected cells under similar conditions. In HEK 293FT cells transfected with the pDualHIV(0) plasmids, the fused *Renilla*-firefly luciferase protein is synthesized by conventional translation rules, i.e. without ribosomal frameshifting. Therefore, to confirm that the observed effect in pDualHIV(−1) cells is a direct effect of compound on frameshift-dependent translation, pDualHIV(0) transfected cells were treated analogously with compounds 4 and 5. No change in Fluc to Rluc ratio relative to untreated pDualHIV(0) transfected HEK 293FT cells was observed, suggesting that 4 and 5 specifically stimulate −1 frameshift translation in cells. Disulfide linked 11 stimulated HIV-1 frameshifting by approximately 25% (Supporting Information); this lower effect compared to the cases of 4 and 5 is consistent with its lower affinity to the HIV-1 FSS and likely lability in the cell. Treatment of HEK 293FT transfected with the pDualHTLV-2 (−1) construct with compounds 4, 5, or 11 resulted in no change in Fluc/Rluc ratio compared to the case of untreated cells. This is consistent with *in vitro* SPR results in which no binding was observed between these compounds and the HTLV-2 FSS RNA.

**Compounds 4 and 5 Decrease Viral Infectivity.** In order for the observed −1 frameshift effect of compounds to be significant, it was important that it correlate to an equivalent reduction in viral replication. To assess this, we analyzed the effect of compounds in a single-round infection with pseudotyped HIV in HEK 293T producer cells and TZM-bl target cells (a HeLa cell line).<sup>46</sup> The wild type HIV proviral vector (pDHIV3-GFP) codes for all HIV-1<sub>NL4-3</sub> genes except *nef* (which is replaced with GFP) and *env*, thus preserving *gag* and *pol*, and the frameshift required for production of the Gag-Pol polyprotein. Preliminary experiments with 2 and 3 showed no activity in this assay. However, we observed a statistically significant ( $p < 0.001$ ) and concentration-dependent decrease in infectivity of the pseudotyped HIV-1 virions when producer cells were treated with 4 and 5 (Figure 5). The decrease in infectivity was >90% at a concentration of 20  $\mu\text{M}$  4, and >90% at a concentration of 40  $\mu\text{M}$  for 5. The core peptide alone (10) showed a modest decrease in infectivity at a concentration of 40

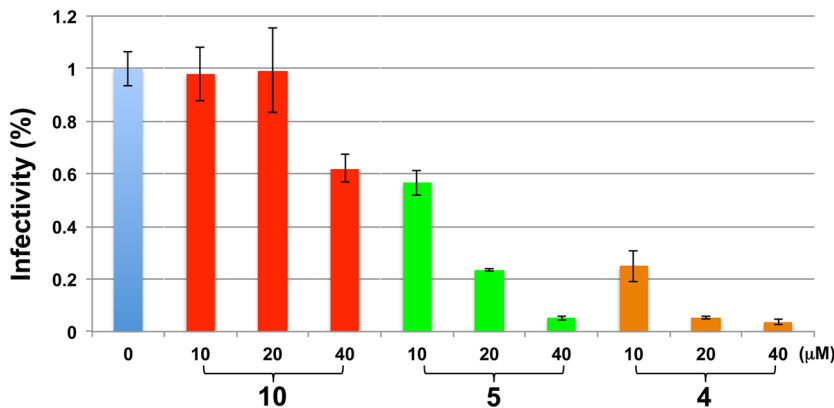


**Figure 5.** Treatment of viral producer cells with compounds 4 and 5 yields a strong inhibition of the infectivity of pseudotyped HIV-1 virions into TZM-bl reporter cells. Infectivity is measured as relative luminescence from the stably expressed firefly luciferase expressed via the HIV LTR promoter in the TZM-bl cell line. Error bars indicate standard deviation on the mean ( $N = 3$ ).

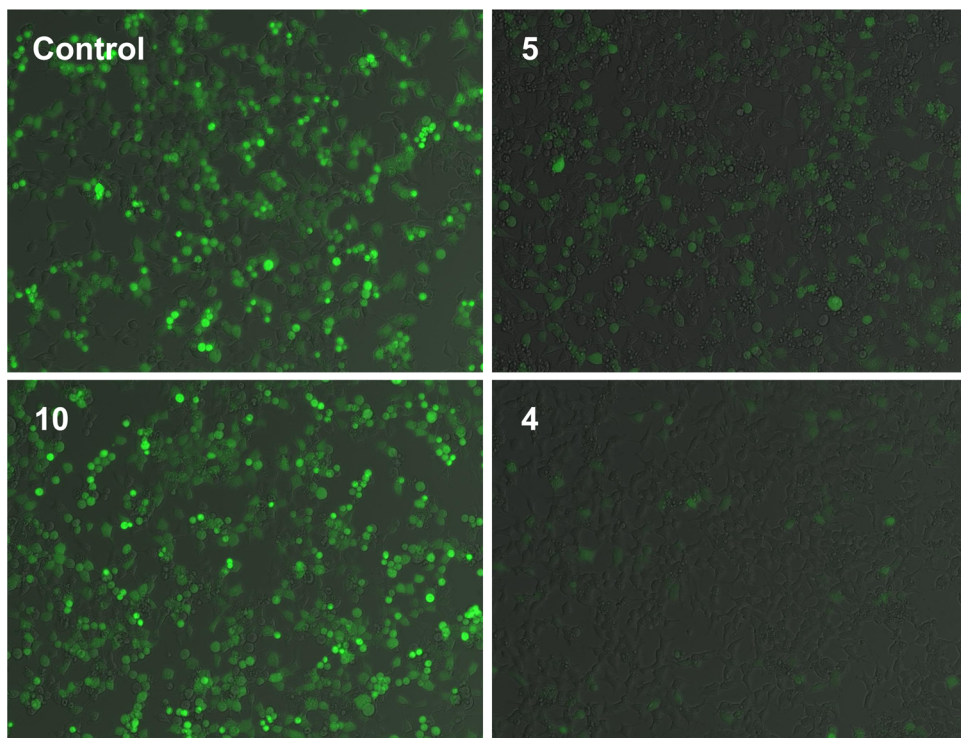


**Figure 6.** Compound-dependent changes in viral production may be observed directly via fluorescence microscopy. Proviral expression of GFP is reduced in the presence of compounds 4 and 5 compared to 10 and the untreated control (40  $\mu\text{M}$  concentration shown). Images were acquired 24 h after treatment prior to harvesting viral particles for TZM-bl single-cycle infectivity.

$\mu\text{M}$ , likely via nonspecific effects, given its lack of affinity for the FSS.  $\text{EC}_{50}$  values for 4 and 5 were 3.9 and 25.6  $\mu\text{M}$ , respectively. The protease inhibitor Indinavir was tested in parallel to calibrate the assay; its  $\text{EC}_{50}$  was found to be 14.8 nM, in line with previously reported values.<sup>47</sup>

While virus titer was determined in these experiments using an ELISA assay to normalize viral load into target cells, a compound-dependent decrease in viral production was also readily observable via fluorescence microscopy, as the pseudotyped HIV carries GFP as a marker (Figure 6). Phase-contrast images of these cells showed no morphological changes, consistent with WST-1 results (Supporting Information). The concentration range required for a decrease in viral infectivity by 4 and 5 was similar to the range at which a significant increase in  $-1$  frameshift was observed in HEK 293

FT cells, supporting the hypothesis that these compounds exert their antiviral activity primarily by altering  $-1$  PRF. In order to provide further support for this hypothesis, viral particles were isolated from supernatants from these experiments by spinning through a 20% sucrose cushion, and probed via Western blot for the presence of reverse transcriptase (RT). As RT is produced only as part of the Gag-Pol fusion, increasing amounts of RT relative to capsid protein p24 (a structural protein produced as part of Gag) would be required given an increase in frameshifting. Indeed, that is what is observed as a function of added 4 or 5 (Figure 7). The amount of RT in unprocessed Gag-Pol (p160) relative to mature RT (p66 + p51) also increased significantly; this may indicate that treatment with compounds 4 and 5 also inhibits Pol processing. However, the pattern of p160 cleavage intermediates observed

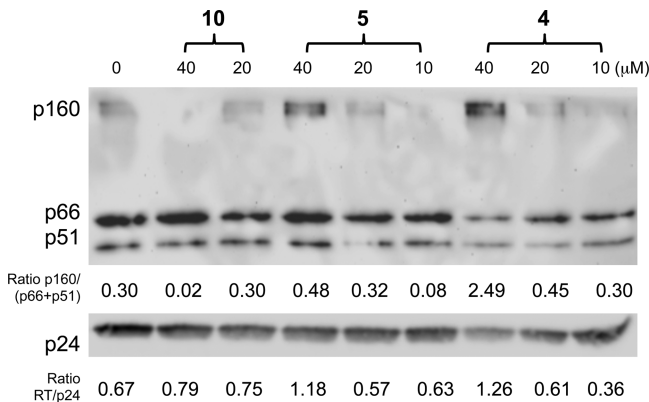


**Figure 7.** Compounds affect Gag:Gag-Pol ratio in pseudotyped virions. Equal loads of viral particles (measured by p24 ELISA) were isolated from media of viral producer cells by spinning through a 20% sucrose cushion at 100,000g. The viral particles were Western blotted for RT (Abcam) and p24 (NIH AIDS Reagent Program, cat #3537). Densitometry of nonsaturated bands was used to calculate ratios for p160/(p66+p51) (listed below the RT blot) and the ratio of total (all bands) RT/p24 are (listed below the p24 blot).

on treatment with Indinavir is significantly different, indicating that 4 and 5 likely do not directly interact with viral protease (Supporting Information p S19).

## ■ DISCUSSION AND CONCLUSIONS

Designing small molecules that target specific RNA sequences and elicit a desired RNA mediated biological response constitutes one of the signature challenges in chemical biology.<sup>48,49</sup> In this paper, we have demonstrated that a moderate-affinity “hit” compound for the HIV-1 FSS RNA, obtained from a resin-bound dynamic combinatorial library screen, can be transformed into high-affinity binders. An intriguing observation from our initial screen<sup>36</sup> was the finding that a symmetrical compound was selected, despite the target RNA being nonsymmetrical. This work confirms that both putative intercalators are required for high-affinity binding, as compounds 7 and 8 had only weak affinity for the FSS. Structural analysis will be essential to fully understand the binding mode of 4 and 5, but the recognition of a nonsymmetrical RNA binding site by a symmetrical, dimeric molecule is not unprecedented; for example, Arya and colleagues have described the use of neomycin dimers for recognition of HIV TAR RNA,<sup>50</sup> and the Hergenrother group designed deoxystreptamine dimers that bound nonsymmetrical RNA loops.<sup>51</sup> Likewise, structural information should prove useful for understanding the significantly higher selectivity of 4 for FSS RNA over FSS DNA and tRNA relative to 5.

These enhanced compounds are able to alter frameshifting in a dual luciferase assay in HEK 293FT cells and strongly inhibit viral infectivity in a pseudotyped HIV assay. Relative to previously studied compounds targeting frameshifting in HIV, compounds 4 and 5 produce a roughly equivalent increase in RT at a 37.5-fold lower concentration than RG501. As such, compounds 4 and 5 represent promising leads for further study, as well as interesting tools to further investigate the mechanism of  $-1$  PRF. Since the pseudotyped HIV used in this assay is only capable of one round of replication, we anticipate that stronger effects will be observed with wild-type HIV in a spreading infection assay. Of course, further enhancements in affinity and selectivity would likely improve activity as well. As

discussed above, previous high-throughput screening efforts targeting frameshift-modulating compounds in which bicistronic reporters provided the assay readout largely yielded compounds acting on the ribosome. Given this observation, it has been suggested by others that assays focused on direct binding to the FSS RNA could be advantageous, as such compounds could potentially increase frameshifting by inhibiting unwinding of the upper stem-loop.<sup>6</sup> The results presented herein support this hypothesis. In the context of HIV biology, our results with compounds 4 and 5 indicate that an increase in frameshifting and a concomitant increase in the Gag-Pol/Gag ratio decreases viral fitness. This is consistent with the work of Mak and colleagues, who increased the Gag-Pol/Gag ratio via cotransfection.<sup>52</sup>

## ■ EXPERIMENTAL SECTION

**Reagents.** Commercially available reagents were obtained from Sigma-Aldrich Chemical Co. (St. Louis, MO), TCI America (Portland, OR), Fisher Scientific, EMID Chemicals (Gibbstown, NJ), Advanced ChemTech (Louisville, KY), and Alfa Aesar, and were used without further purification unless otherwise noted. Water used for reactions and aqueous workup was glass-distilled from a deionized water feed. Reagent grade solvents were used for all nonaqueous extractions. Reaction progress was monitored by analytical thin-layer chromatography (TLC) using EM silica gel 60 F-254 precoated glass plates (0.25 mm). Compounds were visualized on the TLC plates with a UV lamp (dual wavelength;  $\lambda = 254 \text{ nm}$ ,  $\lambda = 360 \text{ nm}$ ). Synthesized compounds were purified using flash column chromatography on EM silica gel 60 (230–400) mesh or alternatively via preparative reversed phase HPLC. Cells were cultured in Dulbecco’s modified Eagle’s medium (DMEM), supplemented with 10% FBS and 1% penicillin–1% streptomycin. Premixed WST-1 cell proliferation reagent was purchased from Clontech, and luminescence assays were carried out using a Promega dual-luciferase assay kit following manufacturer’s instructions.

**Analysis.**  $^1\text{H}$  NMR spectra were recorded at 25 °C on either a Bruker Avance 400 (400 MHz) or Bruker Avance 500 (500 MHz) instrument and processed using MestReNova NMR processing software. Chemical shifts ( $\delta$ ) are reported in parts per million (ppm) downfield from tetramethylsilane and referenced to the residual protium signal in the NMR solvents. Data are reported as follows: chemical shift, multiplicity (s = singlet, d = doublet, t = triplet, m = multiplet, and q = quartet), coupling constant ( $J$ ) in Hertz (Hz), and integration.  $^{13}\text{C}$  spectra were recorded at 25 °C on a Bruker Avance 500 instrument operating at 126 MHz. Chemical shifts ( $\delta$ ) are reported in ppm downfield from tetramethylsilane and referenced (except in  $\text{D}_2\text{O}$ ) to the primary carbon resonance in the NMR solvent. FT-IR spectra were recorded on a Shimadzu FT-IR spectrophotometer. High-resolution mass spectra (HRMS) were acquired at the University of Buffalo Chemistry Department Mass Spectrometry Facility, Buffalo, NY.

**Synthesis of Compounds.** Compounds were synthesized following procedures analogous to those previously reported.<sup>35,37</sup> All compounds were produced in >95% purity, as determined by analytical HPLC. Briefly, 4 and 5 were synthesized from olefin precursor monomer 6, which was assembled on Wang resin by standard Fmoc solid phase peptide synthesis (SPPS) methods. One half of the resin-bound monomer was cleaved using 50% TFA in DCM with 1% TES, and was used as solution phase partner in an olefin metathesis reaction employing Grubbs’ second generation catalyst. The olefin products (isomer ratio of Z/E = 2:3) were isolated using reverse phase HPLC on a C18 column (Waters, XBridge Prep C18 5  $\mu\text{m}$  OBD, 19 mm × 250 mm) using gradient elution from 5 to 100% acetonitrile/0.1% TFA in water/0.1% TFA. Olefin geometries were assigned by comparing the olefin proton chemical shifts of the E-olefin downfield to the Z-isomer and also by the infrared spectra of the compounds as described previously.<sup>37</sup>

Compounds 7 and 8 were synthesized by a slight modification to the procedures described above. The tripeptide (Phe-Pro-AllylGly) was first assembled using Fmoc peptide coupling chemistry on Wang resin. The resin-bound tripeptide was then separated into two equal parts. 2-Ethyl benzo[g]quinoline carboxylic acid was coupled to half the material and cleaved with TFA. This was then employed as the solution phase component in olefin cross-metathesis with the remaining bead-bound portion of Fmoc-protected tripeptide.

**Surface Plasmon Resonance (SPR) Binding Analysis.** Surface plasmon resonance (SPR) experiments were performed on a BIAcore-X instrument (BIAcore, Inc., Uppsala, Sweden) on a CMS sensor chip. Approximately 2000 RU of streptavidin (Rockland Immunochemicals) was immobilized in both flow cells using EDC/NHS chemistry. 5'-Biotinylated-RNA (either 500 nM 5'-biotin-HIV-1 FSS or 500 nM 5'-biotin-HTLV-2 FSS RNA sequences, obtained commercially from Integrated DNA Technologies Inc.) was captured onto the streptavidin surface in one flow cell to a density of approximately 300–1200 RU. The streptavidin surface in the second flow cell was then blocked with biotin solution and served as a reference cell to correct for any nonspecific binding. Binding constant measurements were carried out for each compound once on a “low density” (approximately 300 RU) chip and once on a “high-density” (approximately 1200 RU) chip in order to ensure binding was not influenced by RNA density. Kinetic binding experiments were carried out by flowing various concentrations of compound in (a) HBS buffer (0.01 M HEPES, 0.150 M NaCl, pH = 7.4) at a 60  $\mu$ L per min flow rate or (b) 20 mM HEPES, 150 mM NaCl, 5 mM MgCl<sub>2</sub>, and 0.005% Tween-20 at a 50  $\mu$ L per min flow rate over the captured RNA sequence. Where necessary, a 20 s, 0.5 or 1 M aqueous NaCl injection was sufficient for regeneration (compounds displaying fast off-rates did not require regeneration of the chip between injections). Binding constants were obtained by global fit (conditions (a)) of association and dissociation phases of at least five referenced-subtracted and blank-corrected sensorgrams to a 1:1 Langmuir binding equation, or via individual fits (conditions (b) using BIAevaluation software). Injection of each concentration was repeated at least twice for consistency.

**Fluorescence Titrations.** Fluorescence titrations were carried out in 20 mM HEPES, 150 mM NaCl, using a Cary Eclipse spectrofluorometer. All titrations started at a volume of 500  $\mu$ L with the compound at 1  $\mu$ M. RNA was then titrated in from a high-concentration stock (10  $\mu$ M for HIV-1 FSS RNA; 40  $\mu$ M for HIV-1 FSS DNA and tRNA) in 1–10  $\mu$ L increments. After RNA was added, the solution was thoroughly mixed in the cuvette via pipetting and allowed to stand for 10 min to reach equilibrium. Each measurement was taken three times with a 1 min waiting period between scans to confirm equilibrium was reached. Intensities were corrected for dilution.

**Cell Permeation.** HEK 293FT cells grown to 80% confluence at 37 °C and 5% CO<sub>2</sub> were exposed to compounds at a concentration of 50  $\mu$ M for 12 h in a 96-well tissue culture plate. After removal of the culture media [DMEM containing 10% FBS, 1% penicillin-streptomycin (GIBCO)], the cells were washed twice with PBS to remove excess and surface-bound compounds. Cells were then imaged while in buffer under a fluorescence microscope (Olympus IX70) in the 96-well plate using 358-nm excitation and 460-nm emission filters.

**Cell Toxicity.** HEK 293 FT cells were plated in a 96-well tissue culture plate in DMEM (10% fetal bovine serum, 1% penicillin-streptomycin) and allowed to grow to 80% confluence at 37 °C under CO<sub>2</sub>. Varying compound concentrations (up to 0.5 mM) and control (identical volumes of sterile H<sub>2</sub>O) in triplicate were incubated with cells for 24 h at 37 °C. Ten microliters of Premix WST-1 cell proliferation reagent (Clontech) was added to each well including blanks (DMEM), followed by a 2 h incubation at 37 °C. Absorbances measured at 450 and 690 nm were subtracted and blank corrected. The difference in absorbance was plotted against compound concentration.

**Dual-Luciferase Reporter Frameshift Assay in 293FT Cells.** HEK 293FT cells were plated in 96-well plates at densities of 1.5 × 10<sup>4</sup> cells/well 6 h before transfection in DMEM (10% fetal bovine serum,

1% penicillin-streptomycin). Cells were transiently transfected in separate wells with 0.2  $\mu$ g of plasmid DNA (pDualHIV(0), pDualHIV(-1), pDualHTLV-2(0), or pDualHTLV-2(-1)), using lipofectamine 2000 transfection reagent (Invitrogen) and following the manufacturer's protocol. Five hours after transfection, various compound concentrations (0–50  $\mu$ M) were added directly to the cells in triplicate and incubated for 36 h at 37 °C. The culture media was gently aspirated, washed with 1× PBS, and lysed with 200  $\mu$ L 1× passive lysis buffer. Rluc and Fluc activities were measured with 5  $\mu$ L of cell lysate and 25  $\mu$ L of luciferase reagent using the dual-luciferase assay system (Promega) in the same wells. Fluc and Rluc luminescence values were measured on a Modulus microplate reader (Turner Biosystems). Relative frameshift efficiencies were calculated by comparing the Fluc/Rluc luminescence ratio of cells treated with compounds to untreated cells.

**HIV-1 Infectivity Assay.** The antiviral activity of 4, 5, and 10 was measured by single-round infectivity assay with pseudotyped HIV-1 using HEK293T producer cells. The HIV-1 proviral vector (pDHIV3-GFP) codes for all HIV-1<sub>NL4-3</sub> genes except *nef* (replaced with GFP) and *env*, thus preserving *gag* and *pol*, and the frameshift required for production of the Gag-Pol polyprotein. A single-round infectivity assay was conducted by transient transfection of the viral vector with VSV-G coat protein vector at a ratio of 1:0.5 using Fugene HD (Promega). The virus producer cells were dosed with compounds four hours after transfection, and viral particles were harvested from the media 24 h after transfecting by filtering through a 0.45- $\mu$ m syringe filter. Viral load was normalized with a p24 ELISA (Perkin-Elmer).

The infections were performed using TZM-bl reporter cells that contain stably integrated firefly luciferase that is driven by the HIV-LTR promoter. Therefore, luciferase is expressed upon successful HIV infection.<sup>53</sup> Triplicate infections in 96-well plates at 10,000 cells/well with 500 pg p24/well proceeded for 48 h before the addition of SteadyGlo Reagent (Promega) to each well for 30 min. Luminescence was measured as a quantitative metric for changes in viral infectivity in the presence of compound.

## ASSOCIATED CONTENT

### Supporting Information

Spectroscopic characterization of new compounds, SPR traces, fluorescence titrations, and brightfield images of compound-treated cells from the pseudotyped HIV-1 assay. This material is available free of charge via the Internet at <http://pubs.acs.org>.

## AUTHOR INFORMATION

### Corresponding Author

\*E-mail: Benjamin\_Miller@urmc.rochester.edu. Phone: 585-275-9805.

### Author Contributions

<sup>†</sup>L.O.O., T.A.H., and R.P.B. contributed equally

### Notes

The authors declare no competing financial interest.

## ACKNOWLEDGMENTS

We thank Professor Léa Brakier-Gingras (Université de Montréal) for helpful discussions and for the generous donation of plasmids, and Professor Glynis Scott (University of Rochester) for a generous donation of HEK 293 FT cells. This work was supported in part by the National Institutes of Health: NIGMS Grant R01GM100788 (to B.L.M.), University of Rochester Developmental Center for AIDS Research Grant P30 AI078498 (NIH/NIAID), NIH/NINDS R21 NS067671 (to H.C.S.), and Institutional Ruth L. Kirschstein National Research Service Award GM068411 (T.A.H.). The content is solely the responsibility of the authors and does not necessarily represent the official views of the National Institutes of Health.

## ■ ABBREVIATIONS USED

CEM, human T-cell lymphoblast-like cell line; CH-1, a murine B-cell lymphoma cell line; DMEM, Dulbecco's modified eagle's medium; FBS, fetal bovine serum; Fmoc, fluorenylmethoxy carbonyl; FSS, frameshift stimulating sequence; HAART, highly active antiretroviral therapy; HBS, HEPES buffered saline; HEPES, 2-[4-(2-hydroxyethyl)piperazin-1-yl]ethanesulfonic acid; HIV-1, human immunodeficiency virus type 1; HTLV-2, human T-cell leukemia virus type 2; ORF, open reading frame; PRF, programmed ribosomal frameshifting; RT, reverse transcriptase; RU, response units; SHAPE, selective 2'-hydroxyl acylation analyzed by primer extension; SPPS, solid phase peptide synthesis; SPR, surface plasmon resonance; TAR, trans-activation response element; WST-1, water-soluble tetrazolium salt 1

## ■ REFERENCES

- (1) Fauci, A. S. The human immunodeficiency virus: infectivity and mechanisms of pathogenesis. *Science* **1988**, *239*, 617–622.
- (2) Guyader, M.; Emerman, M.; Sonigo, P.; Clavel, F.; Montagnier, L.; Alizon, M. Genome organization and transactivation of the human immunodeficiency virus type 2. *Nature* **1987**, *326*, 662–669.
- (3) unaids.org/documents/20101123\_GlobalReport\_Chap2\_em.pdf.
- (4) Bangsberg, D. R.; Perry, S.; Charlebois, E. D.; Clark, R. A.; Roberson, M.; Zolopa, A. R.; Moss, A. Non-adherence to highly active antiretroviral therapy predicts progression to AIDS. *AIDS* **2001**, *15*, 1181–1183.
- (5) Saini, S. S.; Bhalla, P. P.; Gautam, H. H.; Baveja, U. K. U.; Pasha, S. T. S.; Dewan, R. R. Resistance-Associated Mutations in HIV-1 among Patients Failing First-Line Antiretroviral Therapy. *J. Int. Assoc. Physicians AIDS Care* **1970**, *11*, 203–209.
- (6) Brakier-Gingras, L.; Charbonneau, J.; Butcher, S. E. Targeting frameshifting in the human immunodeficiency virus. *Expert Opin. Ther. Targets* **2012**, *249*–258.
- (7) Dulude, D.; Berchiche, Y. A.; Gendron, K.; Brakier-Gingras, L.; Heveker, N. Decreasing the frameshift efficiency translates into an equivalent reduction of the replication of the human immunodeficiency virus type 1. *Virology* **2006**, *345*, 127–136.
- (8) Dulude, D.; Baril, M.; Brakier-Gingras, L. Characterization of the frameshift stimulatory signal controlling a programmed –1 ribosomal frameshift in the human immunodeficiency virus type 1. *Nucleic Acids Res.* **2002**, *30*, 5094–5102.
- (9) Brakier-Gingras, L.; Dulude, D. Programmed –1 ribosomal frameshift in the human immunodeficiency virus of type 1. In *Recoding: Expansion of Decoding Rules Enriches Gene Expression*; Atkins, J., Gesteland, R., Eds.; Springer: New York, NY, 2010; pp 175–192.
- (10) Weiss, R. B. R.; Dunn, D. M. D.; Shuh, M. M.; Atkins, J. F. J.; Gesteland, R. F. R. E. coli ribosomes re-phase on retroviral frameshift signals at rates ranging from 2 to 50%. *New Biol.* **1989**, *1*, 159–169.
- (11) Namy, O.; Moran, S. J.; Stuart, D. I.; Gilbert, R. J. C.; Brierley, I. A mechanical explanation of RNA pseudoknot function in programmed ribosomal frameshifting. *Nature* **2006**, *441*, 244–247.
- (12) Léger, M.; Dulude, D.; Steinberg, S. V.; Brakier-Gingras, L. The three transfer RNAs occupying the A, P and E sites on the ribosome are involved in viral programmed –1 ribosomal frameshift. *Nucleic Acids Res.* **2007**, *35*, 5581–5592.
- (13) Telenti, A. A.; Martinez, R. R.; Munoz, M. M.; Bleiber, G. G.; Greub, G. G.; Sanglard, D. D.; Peters, S. S. Analysis of natural variants of the human immunodeficiency virus type 1 gag-pol frameshift stem-loop structure. *J. Virol.* **2002**, *76*, 7868–7873.
- (14) Brierley, I.; Pennell, S. Structure and Function of the Stimulatory RNAs Involved in Programmed Eukaryotic –1 Ribosomal Frameshifting. *Cold Spring Harbor Symp. Quant. Biol.* **2001**, *66*, 233–248.
- (15) Irvine, J. H. J.; Horsfield, J. A. J.; McKinney, C. Z. C.; Tate, W. P. W. A novel strategy to interfere with human immunodeficiency virus type 1 propagation. *N. Z. Med. J.* **1998**, *111*, 222–224.
- (16) Kinzy, T. G. New Targets for Antivirals: The Ribosomal A-Site and the Factors That Interact with It. *Virology* **2002**, *300*, 60–70.
- (17) Kobayashi, Y.; Zhuang, J.; Peltz, S.; Dougherty, J. Identification of a cellular factor that modulates HIV-1 programmed ribosomal frameshifting. *J. Biol. Chem.* **2010**, *285*, 19776–19784.
- (18) Staple, D. W.; Butcher, S. E. Solution structure of the HIV-1 frameshift inducing stem-loop RNA. *Nucleic Acids Res.* **2003**, *31*, 4326–4331.
- (19) Staple, D. W.; Butcher, S. E. Solution structure and thermodynamic investigation of the HIV-1 frameshift inducing element. *J. Mol. Biol.* **2005**, *349*, 1011–1023.
- (20) Gaudin, C.; Mazauric, M.-H.; Traikia, M.; Guittet, E.; Yoshizawa, S.; Fourmy, D. Structure of the RNA Signal Essential for Translational Frameshifting in HIV-1. *J. Mol. Biol.* **2005**, *349*, 1024–1035.
- (21) Sorin, E. J.; Engelhardt, M. A.; Herschlag, D.; Pande, V. S. RNA simulations: probing hairpin unfolding and the dynamics of a GNRA tetraloop. *J. Mol. Biol.* **2002**, *317*, 493–506.
- (22) Watts, J. M.; Dang, K. K.; Gorelick, R. J.; Leonard, C. W.; Bess, J. W.; Swanstrom, R.; Burch, C. L.; Weeks, K. M. Architecture and secondary structure of an entire HIV-1 RNA genome. *Nature* **2009**, *460*, 711–716.
- (23) Low, J. T.; Weeks, K. M. SHAPE-directed RNA secondary structure prediction. *Methods* **2010**, *52*, 150–158.
- (24) Brierley, I.; Ramos Dos, F. J. Programmed ribosomal frameshifting in HIV-1 and the SARS-CoV. *Virus Res.* **2006**, *119*, 29–42.
- (25) Kim, Y. G. Y.; Maas, S. S.; Rich, A. A. Comparative mutational analysis of cis-acting RNA signals for translational frameshifting in HIV-1 and HTLV-2. *Nucleic Acids Res.* **2001**, *29*, 1125–1131.
- (26) Falk, H. H.; Mador, N. N.; Udi, R. R.; Panet, A. A.; Honigman, A. A. Two cis-acting signals control ribosomal frameshift between human T-cell leukemia virus type II gag and pro genes. *J. Virol.* **1993**, *67*, 6273–6277.
- (27) Hung, M.; Patel, P.; Davis, S.; Green, S. R. Importance of ribosomal frameshifting for human immunodeficiency virus type 1 particle assembly and replication. *J. Virol.* **1998**, *72*, 4819–4824.
- (28) Babé, L. M.; Craik, C. S. Constitutive production of nonenveloped human immunodeficiency virus type 1 particles by a mammalian cell line and effects of a protease inhibitor on particle maturation. *Antimicrob. Agents Chemother.* **1994**, *38*, 2430–2439.
- (29) Marcheschi, R. J.; Tonelli, M.; Kumar, A.; Butcher, S. E. Structure of the HIV-1 frameshift site RNA bound to a small molecule inhibitor of viral replication. *ACS Chem. Biol.* **2011**, *6*, 857–864.
- (30) Staple, D. W.; Venditti, V.; Niccolai, N.; Elson-Schwab, L.; Tor, Y.; Butcher, S. E. Guanidinoneomycin B recognition of an HIV-1 RNA helix. *ChemBioChem* **2008**, *9*, 93–102.
- (31) Marcheschi, R. J.; Mouzakis, K. D.; Butcher, S. E. Selection and characterization of small molecules that bind the HIV-1 frameshift site RNA. *ACS Chem. Biol.* **2009**, *4*, 844–854.
- (32) Dulude, D.; Théberge-Julien, G.; Brakier-Gingras, L.; Heveker, N. Selection of peptides interfering with a ribosomal frameshift in the human immunodeficiency virus type 1. *RNA* **2008**, *14*, 981–991.
- (33) Karan, C. C.; Miller, B. L. B. RNA-selective coordination complexes identified via dynamic combinatorial chemistry. *J. Am. Chem. Soc.* **2001**, *123*, 7455–7456.
- (34) McNaughton, B. R.; Miller, B. L. Resin-bound dynamic combinatorial chemistry. *Org. Lett.* **2006**, *8*, 1803–1806.
- (35) Palde, P. B.; Ofori, L. O.; Gareiss, P. C.; Lerea, J.; Miller, B. L. Strategies for recognition of stem-loop RNA structures by synthetic ligands: application to the HIV-1 frameshift stimulatory sequence. *J. Med. Chem.* **2010**, *53*, 6018–6027.
- (36) McNaughton, B. R.; Gareiss, P. C.; Miller, B. L. Identification of a Selective Small-Molecule Ligand for HIV-1 Frameshift-Inducing Stem-Loop RNA from an 11,325 Member Resin Bound Dynamic Combinatorial Library. *J. Am. Chem. Soc.* **2007**, *129*, 11306–11307.

- (37) Ofori, L. O.; Hoskins, J.; Nakamori, M.; Thornton, C. A.; Miller, B. L. From dynamic combinatorial “hit” to lead: in vitro and in vivo activity of compounds targeting the pathogenic RNAs that cause myotonic dystrophy. *Nucleic Acids Res.* **2012**, *40*, 6380–6390.
- (38) Davis, T. M.; Wilson, W. D. Surface plasmon resonance biosensor analysis of RNA-small molecule interactions. *Meth. Enzymol.* **2001**, *340*, 22–51.
- (39) Rich, R. L.; Myszka, D. G. Survey of the 2009 commercial optical biosensor literature. *J. Mol. Recognit.* **2011**, *24*, 892–914.
- (40) Giannetti, A. M.; Koch, B. D.; Browner, M. F. Surface plasmon resonance based assay for the detection and characterization of promiscuous inhibitors. *J. Med. Chem.* **2008**, *51*, 574–580.
- (41) Luedtke, N. W.; Carmichael, P.; Tor, Y. Cellular uptake of aminoglycosides, guanidinoglycosides, and poly-arginine. *J. Am. Chem. Soc.* **2003**, *125*, 12374–12375.
- (42) Buttke, T. M. T.; McCubrey, J. A. J.; Owen, T. C. T. Use of an aqueous soluble tetrazolium/formazan assay to measure viability and proliferation of lymphokine-dependent cell lines. *J. Immunol. Methods* **1993**, *157*, 233–240.
- (43) Grentzmann, G.; Ingram, J. A.; Kelly, P. J.; Gesteland, R. F.; Atkins, J. F. A dual-luciferase reporter system for studying recoding signals. *RNA* **1998**, *4*, 479–486.
- (44) Falk, H. H.; Mador, N. N.; Udi, R. R.; Panet, A. A.; Honigman, A. A. Two cis-acting signals control ribosomal frameshift between human T-cell leukemia virus type II gag and pro genes. *J. Virol.* **1993**, *67*, 6273–6277.
- (45) Kim, Y. G. Y.; Maas, S. S.; Rich, A. A. Comparative mutational analysis of cis-acting RNA signals for translational frameshifting in HIV-1 and HTLV-2. *Nucleic Acids Res.* **2001**, *29*, 1125–1131.
- (46) Miller, J. H.; Presnyak, V.; Smith, H. C. The dimerization domain of HIV-1 viral infectivity factor Vif is required to block virion incorporation of APOBEC3G. *Retrovirology* **2007**, *4*, 81.
- (47) Zhang, L.; Gorset, W.; Washington, C. B.; Blaschke, T. F.; Kroetz, D. L.; Giacomini, K. M. Interactions of HIV protease inhibitors with a human organic cation transporter in a mammalian expression system. *Drug Metab. Dispos.* **2000**, *28*, 329–334.
- (48) Guan, L.; Disney, M. D. Recent advances in developing small molecules targeting RNA. *ACS Chem. Biol.* **2012**, *7*, 73–86.
- (49) Thomas, J. R.; Hergenrother, P. J. Targeting RNA with Small Molecules. *Chem. Rev.* **2008**, *108*, 1171–1224.
- (50) Kumar, S. S.; Kellish, P. P.; Robinson, W. E. W.; Wang, D. D.; Appella, D. H. D.; Arya, D. P. D. Click dimers to target HIV TAR RNA conformation. *Biochemistry* **2012**, *51*, 2331–2347.
- (51) Thomas, J. R. J.; Liu, X. X.; Hergenrother, P. J. P. Size-specific ligands for RNA hairpin loops. *J. Am. Chem. Soc.* **2005**, *127*, 12434–12435.
- (52) Shehu-Xhilaga, M.; Crowe, S. M.; Mak, J. Maintenance of the Gag/Gag-Pol ratio is important for human immunodeficiency virus type 1 RNA dimerization and viral infectivity. *J. Virol.* **2001**, *75*, 1834–1841.
- (53) Platt, E. J. E.; Wehrly, K. K.; Kuhmann, S. E. S.; Chesebro, B. B.; Kabat, D. D. Effects of CCR5 and CD4 cell surface concentrations on infections by macrophagotropic isolates of human immunodeficiency virus type 1. *J. Virol.* **1998**, *72*, 2855–2864.